



Conditions and extent of volatile loss from the Moon during formation of the Procellarum basin

Romain Tartèse^{a,1} , Paolo A. Sossi^b , and Frédéric Moynier^c

^aDepartment of Earth and Environmental Sciences, The University of Manchester, M13 9PL Manchester, United Kingdom; ^bInstitute of Geochemistry and Petrology, ETH Zürich, CH-8092 Zürich, Switzerland; and ^cUniversité de Paris, Institut de Physique du Globe de Paris, CNRS UMR 7154, 75005 Paris, France

Edited by Mark Thiemens, University of California, San Diego, La Jolla, CA, and approved January 26, 2021 (received for review November 4, 2020)

Rocks from the lunar interior are depleted in moderately volatile elements (MVEs) compared to terrestrial rocks. Most MVEs are also enriched in their heavier isotopes compared to those in terrestrial rocks. Such elemental depletion and heavy isotope enrichments have been attributed to liquid–vapor exchange and vapor loss from the protolunar disk, incomplete accretion of MVEs during condensation of the Moon, and degassing of MVEs during lunar magma ocean crystallization. New Monte Carlo simulation results suggest that the lunar MVE depletion is consistent with evaporative loss at $1,670 \pm 129$ K and an oxygen fugacity $+2.3 \pm 2.1$ log units above the fayalite-magnetite-quartz buffer. Here, we propose that these chemical and isotopic features could have resulted from the formation of the putative Procellarum basin early in the Moon's history, during which nearside magma ocean melts would have been exposed at the surface, allowing equilibration with any primitive atmosphere together with MVE loss and isotopic fractionation.

lunar volatiles | the Moon | Procellarum KREEP Terrane | lunar samples | stable isotopes

Returned samples of basaltic rocks from the Moon provided evidence decades ago that the Moon is depleted in volatile elements compared to the Earth (1), with lunar basalt abundances of moderately volatile elements (MVEs) being $\sim 1/5$ that of terrestrial basalt abundances for alkali elements and $\sim 1/40$ for other MVE, such as Zn, Ag, In, and Cd (2). The theme of lunar volatiles thus seemed settled. Yet, the unambiguous detection in 2008 of lunar indigenous hydrogen and other volatile elements, such as F, Cl, and S in pyroclastic glasses (3), heralded a new era of research into lunar volatiles, overturning the decades-old paradigm of a bone-dry Moon (e.g., refs. 4 and 5). Here, we define volatile elements as those with 50% condensation temperatures below these of the major rock-forming elements Fe, Mg, and Si (6). This paradigm shift was accompanied by new measurements of volatile stable isotope compositions (e.g., H, C, N, Cl, K, Cr, Cu, Zn, Ga, Rb, and Sn) in a wealth of bulk lunar samples (7–18) and in the mineral phases and melt inclusions they host (19–28). These studies have shown that the stable isotope compositions of most MVEs (e.g., K, Zn, Ga, and Rb) are enriched in their heavier isotopes with respect to the bulk silicate Earth (BSE) (9, 11, 13–15, 17). Such heavy isotope enrichment is associated with elemental depletion, which has been variously attributed to liquid–vapor exchange and vapor loss from the protolunar disk (17, 18), incomplete accretion of MVEs during condensation of the Moon (13, 29, 30), and degassing of these elements during lunar magma ocean crystallization (9, 11, 14, 15, 25, 31). Almost all these hypotheses have typically assumed that the MVE depletions and associated MVE isotope fractionations are relevant to the whole Moon. However, our lunar sample collections are biased, as all Apollo and Luna returned samples come from the lunar nearside from within or around the anomalous Procellarum KREEP Terrane (PKT) region (e.g., ref. 32), where KREEP stands for enriched in K, REEs, and P. Barnes et al. (26) proposed that the heavy Cl isotope signature measured in KREEP-rich Apollo samples resulted from metal-chloride degassing from late-stage lunar

magma ocean melts in response to a large crust-breaching impact event, spatially associated with the PKT region, which facilitated exposure of these late-stage melts to the lunar surface. Here, we further investigate whether a localized impact event could have been responsible for the general MVE depletion and heavy MVE isotope enrichment measured in lunar samples.

Volatility, Evaporation Temperature, and MVE Depletion

Volatility is usually quantified as the temperature at which 50% of an element condenses ($50\% T_c$) from a gas phase of solar composition at 10^{-4} bar (6), in which the MVEs are defined as having $50\% T_c$ (K) $< 1,300$ K. This classification has been widely used with the aim of constraining the geological processes by which volatile elements are fractionated among asteroidal and planetary bodies (33, 34). However, these condensation temperatures are strictly only relevant to the evaluation of fractionation processes that took place from a gas phase in the solar nebula and not to address questions related to asteroidal and planetary body formation and differentiation (35). This is because the volatility of an element is partly dependent on the thermodynamic conditions under which volatile depletion occurs, notably the fugacity of oxygen (fO_2) and other major gases, and the phases (solid and liquid) involved in the chemical reactions that take place (e.g., refs. 35–37).

Calculated $50\% T_c$ depend on the Solar System abundances of the elements considered and should thus be reevaluated when Solar System abundance estimates change. Recently, Clay et al. (38) significantly revised down the halogen abundances in Ivunaitype (CI) carbonaceous chondrites (e.g., $\sim 115 \mu\text{g} \cdot \text{g}^{-1}$ versus

Significance

The depletion of moderately volatile elements in the lunar interior, compared to the Earth's interior, is accompanied by enrichment in heavy isotopes for most species. This has been explained by vapor loss from the protolunar disk, incomplete accretion of volatiles, or volatile degassing during crystallization of the lunar magma ocean. Importantly, these hypotheses have assumed that volatile depletion and associated isotope fractionations are relevant to the whole Moon. However, our lunar sample collections are biased, as Apollo and Luna samples come from within or around the anomalous Procellarum KREEP Terrane region on the lunar nearside. Here, we propose that these chemical and isotopic features could have resulted from a large-scale impact event on the nearside early in the Moon's history.

Author contributions: R.T. designed research; R.T. and P.A.S. performed research; R.T., P.A.S., and F.M. analyzed data; and R.T., P.A.S., and F.M. wrote the paper.

The authors declare no competing interest.

This article is a PNAS Direct Submission.

Published under the PNAS license.

¹To whom correspondence may be addressed. Email: romain.tartese@manchester.ac.uk.

This article contains supporting information online at <https://www.pnas.org/lookup/suppl/doi:10.1073/pnas.2023023118/-DCSupplemental>.

Published March 15, 2021.

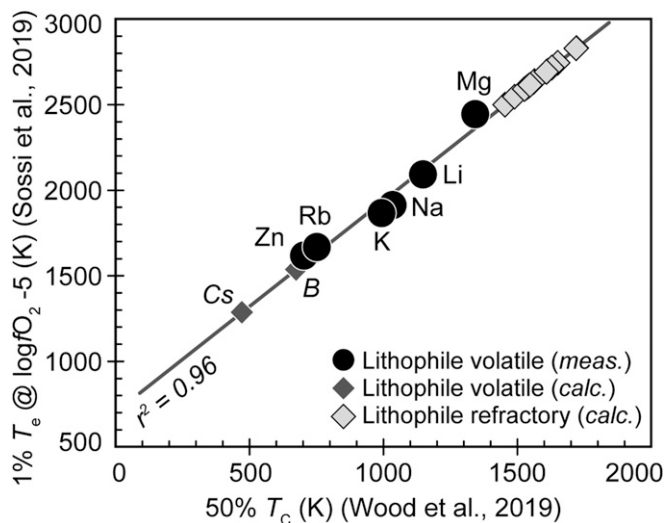


Fig. 1. Comparison of calculated condensation and evaporation temperatures. 1% evaporation temperatures (T_e) determined at 1 bar and $\log f_{O_2-5}$ by Sossi et al. (35) versus 50% T_c determined by Wood et al. (39) for lithophile elements (measured [meas.] corresponds to elements directly determined by Sossi et al. (35); calculated [calc.] corresponds to 1% T_e calculated from the relationship defined by those volatiles with measured 1% T_e and 50% T_c).

$562 \pm 204 \mu\text{g} \cdot \text{g}^{-1}$ for Cl, for example), and new condensation temperature calculations that incorporated these updated Solar System abundance estimates (39) generally agree to within $\pm 5\%$ relative to those calculated by Lodders (6) for refractory elements and main components. The most significant change is for Cl, which was calculated to remain in the gas phase to lower temperatures such that its 50% T_c , calculated by Wood et al. (39), is some 500 K lower (472 K) compared to the estimate of 948 K of Lodders (6).

Complementary to this, Sossi et al. (35) carried out evaporation experiments of MVE from silicate liquids at 1 atmosphere and oxygen fugacities ranging from the Fe-FeO buffer to air (i.e., at conditions more directly relevant to rocky planetary body accretion and early geological evolution). The 1% evaporation temperatures (1% T_e) determined by Sossi et al. (35) for lithophile volatile elements are well correlated with the nebular 50% T_c of Wood et al. (39) but shifted to higher temperatures because of the higher pressure and f_{O_2} (Fig. 1). For lithophile elements not investigated experimentally by Sossi et al. (35), we used the relationship displayed in Fig. 1 to estimate their 1% T_e (SI Appendix, Table S1).

Revised Volatility Trends for the Terrestrial and Lunar Silicate Interiors

These updated 50% T_c (39) and the new evaporation scale, defined as 1% T_e (35), prompted us to reevaluate the MVE depletion pattern for the bulk lunar mantle (BLM). We used the 1% T_e determined at $\log f_{O_2-5}$ (35) since these are close to the fayalite-magnetite-quartz (FMQ) buffer at 1,600 to 1,800 K, conditions that may have prevailed during volatile degassing from a crystallizing lunar magma ocean (16). The elemental abundances used for CI chondrites, the BSE, and the BLM are given in SI Appendix, Table S1. For the BLM, we used the compilation of Hauri et al. (4) for refractory elements and recent estimates derived by Ni et al. (27) from melt inclusion analyses for the volatile elements Na, K, Li, Cu, Zn, Ga, Rb, and Cs. Where available, we selected melt inclusion-derived volatile abundances over those estimated from analyses of pyroclastic glasses and bulk mare basalts, as these might have been affected by volatile degassing upon ascent and emplacement at the lunar

surface (e.g., ref. 40). Note that our calculated BLM Ga abundance differs from that of Ni et al. (27) who estimated $0.57 \mu\text{g} \cdot \text{g}^{-1}$ Ga based on the Ga/Lu ratio measured in a melt inclusion in pyroclastic glass sample 74220. However, Lu and Ga abundances in various 74220 glass fractions show that Ga/Lu ratios correlate with Ga abundance (41), which precludes use of the Ga/Lu ratio to estimate the BLM Ga abundance. On the other hand, the Ga/Al ratios of green and orange pyroclastic glasses are broadly consistent around $7.6 (\pm 2.1) \times 10^{-5}$ for Ga abundances between 2.4 and $5.2 \mu\text{g} \cdot \text{g}^{-1}$ (42), suggesting that using Ga/Al ratios yield a more robust estimate for the Ga abundance in the BLM. Using the Al and Ga concentrations of 4.3 wt% and $5.8 \pm 0.6 \mu\text{g} \cdot \text{g}^{-1}$, respectively, measured in 74220 melt inclusion (27), yields a Ga/Al ratio of 1.35×10^{-4} , corresponding to a Ga abundance in the BLM of $3.2 \pm 0.3 \mu\text{g} \cdot \text{g}^{-1}$.

We have excluded S and the halogens (F, Cl, Br, and I) for constructing the volatile depletion trends. As they dissolve as anions in melts, the dependence of their volatilities on f_{O_2} and melt composition is poorly known, and it is hard to justify that they would behave predictably in planetary systems based on their nebular T_c . We have also excluded the “ice-forming” elements H, C, and N for constructing volatile depletion trends since estimating their bulk abundances in planetary bodies is not trivial. On the Moon, for instance, abundances of H, C, and N can be easily modified by numerous processes (e.g., diffusion, degassing, assimilation of solar wind-enriched soils, and spallation reactions), and these elements are the most prone to terrestrial contamination (see ref. 5 and references therein).

Abundances of lithophile volatile elements in the BSE and the BLM correlate well with 1% T_e determined at 1 atmosphere and $\log f_{O_2-5}$. The BLM is depleted in volatile elements compared to CI chondrites and to the BSE (Fig. 2; SI Appendix, Table S1), a fact that was recognized soon after lunar samples were brought back by the Apollo missions (1, 2). Abundances of B and Cu in the BLM are 3 to 4 times lower than in the BSE; for the alkali elements Na, K, Rb, and Cs, BLM abundances are ~ 5 to 8 times lower than in the BSE, while other MVEs, such as Li, Cr, and Ga, are only negligibly to slightly depleted in the BLM compared to the BSE (Fig. 2). On the other hand, the Zn abundance in the BLM is ~ 20 times lower than in the BSE (Fig. 2).

As tempting as it is, extending these lithophile volatile element depletion trends to lower 1% T_e to estimate the H_2O , C, and N abundances in the BLM and the BSE is not straightforward and

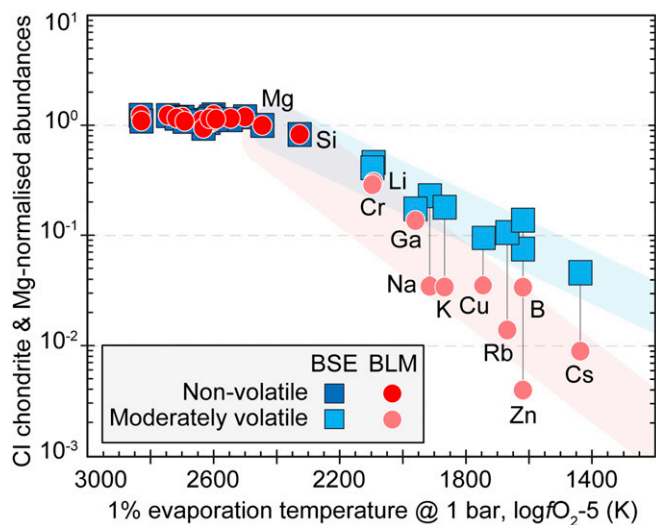


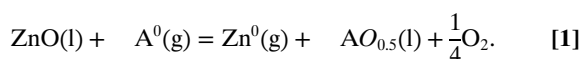
Fig. 2. CI chondrite and Mg-normalized BSE and BLM element abundances versus 1% evaporation temperatures. Element abundances and 1% evaporation temperatures are given in SI Appendix, Table S1.

could yield spurious abundance estimates. This is because the abundance of these atmophile elements in the terrestrial and lunar magma oceans (LMO) would have been largely controlled by their speciation in the liquid and vapor phases and the composition of the overlying atmospheres in equilibrium with these magma oceans (43, 44).

Estimating T and fO_2 Conditions during MVE Volatilization

Displaying the MVE depletion of the BLM with respect to elemental condensation and/or evaporation temperatures (Fig. 2) provides qualitative evidence for elemental depletion having been controlled by volatility but is difficult to reconcile with physical processes expected to have contributed to the formation and geological evolution of the Moon. Such a representation makes physical sense for small, centimeter-sized grains condensing from the solar nebula, for which volatile depletion is not subject to atmospheric escape and occurs in direct response to monotonic cooling of the nebular gas and its nearly instantaneous segregation from condensed phases. However, such a scenario may not apply to the Moon, as its significant mass (1% that of the Earth) requires gaseous molecules to travel at $2.38 \text{ km} \cdot \text{s}^{-1}$ (the present-day escape velocity v_{esc} of the Moon) in order to escape its gravitational pull, assuming it exists as an isolated body in space. As such, there is expected to have been a critical “shut-off” temperature at which volatile depletion becomes negligible because of lack of thermal energy to drive atmospheric escape (e.g., refs. 45 and 46). It has been proposed that the lunar MVE budget has been severely affected by degassing of LMO melts following a single giant impact event (e.g., refs. 16 and 26), during which volatile escape would have occurred over a small temperature range rather than over a longer protracted cooling and condensation interval. Thus, it is crucial to evaluate whether a single combination of T and fO_2 can reproduce the BLM/BSE depletion pattern observed for MVE.

Because the physical conditions for volatile escape from the proto-Moon are complex and depend on many factors, including atmospheric structure and escape regime, we consider the relative depletion of the MVEs with respect to Zn. We chose Zn because its abundance in lunar rocks is well constrained (e.g., ref. 47), it remains lithophile under the conditions of core formation on the Moon (48–50), and it adheres to a simple and well-characterized vaporization behavior from silicate melts (35, 51). Moreover, because it exists as Zn^{2+} in silicate melts, its vaporization stoichiometry differs from those of the alkalis (A^+), such that precise constraints on fO_2 are best evaluated by fixing Zn abundances, via exchange reactions of the following type,



The benefit of this approach is that physical factors affecting absolute elemental losses by evaporation cancel such that the depletion of an element, E , with respect to Zn, may be written as (see ref. 35 and their equation 19)

$$\frac{\ln\left(\frac{X_E^{\text{BLM}}}{X_E^{\text{BSE}}}\right)}{\ln\left(\frac{X_{\text{Zn}}^{\text{BLM}}}{X_{\text{Zn}}^{\text{BSE}}}\right)} = \frac{K_E^*}{K_{\text{Zn}}^*} \cdot fO_2 \cdot \frac{\Delta(n_{\text{Zn}-E})}{4} \cdot \sqrt{\frac{M_{\text{Zn}}}{M_E}}, \quad [2]$$

where X is the mole fraction, M is the molar mass of the evaporating species, n is the number of electrons exchanged in the vaporization reaction (e.g., $n = 2$ for $\text{Zn}^{2+}\text{O(l)} = \text{Zn}^0(\text{g}) + 1/2 \text{O}_2$), and K^* is the modified equilibrium constant of vaporization. This is related to the free energy change of the reaction, ΔG^* , by

$$\Delta G^* = -RT \cdot \ln K^*. \quad [3]$$

Taking one bar as the pressure at standard state, then $\Delta G^* = \Delta H^* - T\Delta S^*$ (H = enthalpy; S = entropy), the values of which are tabulated in Table 5 of Sossi et al. (35). In addition to the presumption that the free energies of these vaporization reactions, which are determined from evaporation of ferrobaltic melts, are applicable to that of a lunar silicate liquid, it also implies low fugacities of Cl_2 and S_2 , which could otherwise bond with metal-bearing gas species (52). In order to account for the uncertainties in the values of ΔH^* and ΔS^* , determined by Sossi et al. (35), we performed Monte Carlo simulations in which the tabulated values of enthalpy and entropy of the vaporization reactions of Mg, Ga, Li, Cu, Na, K, and Rb are associated with conservative $\pm 2.5\%$ relative SD. Eq. 2 is then solved simultaneously for each element, given a fixed $\frac{X_{\text{Zn}}^{\text{BLM}}}{X_{\text{Zn}}^{\text{BSE}}} = 0.052$ (Table 1) in

order to satisfy the constraint of minimization by nonlinear least squares to the observed depletions of the remaining seven elements by varying temperature and fO_2 . This simulation was performed 1,000 times to provide a statistically robust estimate for the best-fit temperatures and oxygen fugacities of evaporation that reproduce the lunar element depletion pattern.

The Monte Carlo simulations yield an average T of MVE depletion of $1,670 \pm 129 \text{ K}$ (1 SD) at an average fO_2 of FMQ $+2.3 \pm 2.1$ (1 SD) (Fig. 3A). Note that these conditions are likely to represent averages integrated over the cooling timescale for the protolunar disk or atmosphere, which may occur over a period of $\sim 10^3$ to 10^4 yr (e.g., ref. 45). These estimates are remarkably consistent with the temperature of 1,600 to 1,800 K and fO_2 near the FMQ buffer required to explain the differences in Cr abundance and stable isotopic composition between the BLM and the BSE (16).

Such oxidizing conditions may appear exceedingly high, as they are at least ~ 3 to 4 orders of magnitude higher than fO_2 estimates of around 1 log unit below the iron-wüstite (IW) buffer deduced from mare basalt petrogenesis and from element partitioning behavior in the lunar interior (e.g., ref. 53). As an intensive property of the system (e.g., rock or magma), fO_2 is uniquely defined by the activities of its constituent phases, pressure, and temperature. Thus, there is no prerequisite that the fO_2 at the surface of a LMO or melt pool should reflect that of mare magmas. Should core formation have buffered the oxygen fugacity at the surface, values near $\sim \text{IW}-1$ would have been expected (53). However, if evaporation took place from a magma ocean that was not fully molten or had experienced partial crystallization, Fe^{3+} abundance could have increased in the residual LMO melts through early olivine precipitation, causing fO_2 to increase, all else being equal. This is consistent with results of a recent study that shows that the $\text{Fe}^{3+}/\Sigma\text{Fe}$ ratios of plagioclase in anorthosites, which are believed to represent solidification products of LMO melts after ~ 70 to 80% crystallization (54), are higher than in plagioclase in any other lunar lithology (55). In addition, elevated fO_2 during volatile degassing is consistent with experimental evaporation of Apollo 12 mare basalts in a Knudsen cell, from which the fO_2 measured by mass spectrometry in the vapor was just above the FMQ buffer at 1,400 to 1,500 K (56). Thermochemical equilibrium calculations also indicate that vapor in equilibrium with a bulk silicate Moon composition would have $fO_2 \sim 3$ log units above the IW buffer at 1,800 K (57).

The BLM/BSE depletion factors (noted as f) calculated for this T - fO_2 combination are consistent with sample-based estimates for Mg, Na, Cu, K, Rb, and Zn (Table 1 and Fig. 3B). In detail, these calculated depletion factors show that Mg is never lost by evaporation, retaining $>99.95\%$ of its initial abundance in all simulations. Averages for the alkali metals and copper bracket their observed values, where $f\text{Cu} = 0.37 \pm 0.02$, $f\text{K} = 0.19 \pm 0.02$,

Table 1. The depletion factors (*f*) of selected MVE and Mg in the BLM relative to the BSE

Element	Mg	Ga	Li	Na	Cu	K	Rb	Zn*
Measured	1.00 [†]	0.8 ± 0.1	0.7 ± 0.3	0.15	0.37	0.19	0.13	0.052
Modeled	1.00 ^{+0.00} _{-0.00}	0.99 ^{+0.01} _{-0.02}	0.98 ^{+0.02} _{-0.03}	0.15 ^{+0.02} _{-0.02}	0.37 ^{+0.02} _{-0.02}	0.19 ^{+0.02} _{-0.02}	0.13 ^{+0.02} _{-0.02}	0.052

"Measured" denotes those inferred from sample-based analyses (*SI Appendix, Table S1*), and "Modeled" shows the average depletion factors obtained from 1,000 Monte Carlo simulations.

*Fixed at the observed value (Eq. 1).

[†]Used as normalizing element for sample-based abundances.

$f_{\text{Na}} = 0.15 \pm 0.02$, and $f_{\text{Rb}} = 0.13 \pm 0.02$. Although alkali metal depletions are unambiguous recorders of volatile loss because of their affinity for the silicate phase over metal during core formation, Cu, particularly for high S contents in the metal, can behave as a siderophile element (58). Nevertheless, the observed Cu depletion can be quantitatively reproduced through vapor loss alone. On the other hand, these calculations predict that Ga and Li are lost only to very minor extents by evaporation ($f_{\text{Ga}} = 0.99^{+0.01}_{-0.02}$, $f_{\text{Li}} = 0.98^{+0.02}_{-0.03}$), with only 4 and 25 simulations resulting in f_{Ga} and $f_{\text{Li}} < 0.9$, respectively. These values exceed sample-based estimates, which yield f_{Ga} of 0.8 ± 0.1 and f_{Li} of 0.7 ± 0.3 . The Li estimate of $1.1 \mu\text{g} \cdot \text{g}^{-1}$ for the BLM is associated with a large uncertainty of $\pm 0.5 \mu\text{g} \cdot \text{g}^{-1}$ (27), indicating that, within uncertainty, sample-based estimates for the BLM could be consistent with the BSE Li abundance of $1.6 \mu\text{g} \cdot \text{g}^{-1}$. The absence of Li loss from the BLM predicted by our modeling is consistent with previous suggestions that Li does not behave as a volatile element during the formation of the Moon (59, 60). As suggested by O'Neill (59), we find that Ga is scarcely volatile under the conditions that best explain the depletion of the other MVEs. This is a function of the strong dependence of the vapor pressure of its presumed predominant gas species above silicate melts, Ga^0 , on f_{O_2} , with an $n = 3$ reaction favoring evaporation under reducing conditions, whereas best fits occur at relatively high f_{O_2} ($\sim \text{FMQ}$). Other potential species (Ga_2O and GaO), which are not considered here, may also become important under oxidizing conditions, promoting Ga loss. We emphasize that the lack of direct measurements of vapor pressures for these species above silicate melts limits our ability to accurately predict the extent of Ga vaporization at present. Indeed, stable isotopic evidence (14) indicates some degree of evaporative loss of Ga from the Moon. On the other hand, simulations of core formation also suggest that the observed Ga depletion in the BLM can be satisfactorily explained by metal-silicate partitioning (e.g., ref. 61). Therefore, better constraints on possible Ga partitioning and vaporization reactions are thus required to distinguish between the relative influence of

these two processes and their importance for the Ga budget of the BLM. It should be noted that the derivation of temperature and f_{O_2} from lunar mantle abundances of MVEs is contingent upon knowledge of their speciation in an early lunar atmosphere. Should "dry" conditions have prevailed, that is, without significant quantities of water and other major volatile species that can bond with the MVEs, such as Cl and S, then they would have vaporized as monatomic gases, as suggested by thermodynamic calculations of lunar magmatic vapors (52). In this case, the foregoing exercise should provide accurate estimations of temperature and oxygen fugacity.

The Stable Isotope Composition of MVEs in the BLM

Incomplete loss or condensation of volatiles during planetary accretion is expected to be accompanied by mass-dependent isotopic fractionation. For refractory elements with 1% T_e higher than Li, the BSE and the BLM have similar stable isotope compositions (Fig. 4A and *SI Appendix, Table S2*). However, the BSE and BLM stable isotope compositions differ for MVEs, the magnitude of difference being related to their 1% T_e (Fig. 4A and *SI Appendix, Table S2*). The elements Li, Ga, K, Cu, Rb, B, and Zn define a rough trend of increasing isotopic fractionation with decreasing 1% T_e (Fig. 4A). This suggests that the bulk of the isotopic difference between the BSE and the BLM for these MVEs might have been established in response to a single large-scale process, related either to incomplete condensation of volatiles in material that accreted to form the Moon after the giant impact, or to loss of volatiles from the Moon-forming disk (9, 17, 18) or the LMO either before a crust formed or through puncturing the early crust and exposing the LMO (e.g., refs. 11, 13–15, 26, 31, 62). Models invoking incomplete condensation as the cause for K and Rb depletion in the BLM (29, 30) are not consistent with the measured K and Rb isotopic difference between the BLM and the BSE, as 1) vapor/condensate equilibrium isotopic fractionation is too small at the temperatures involved ($\sim 3,500$ K) and 2) kinetic isotopic fractionation would

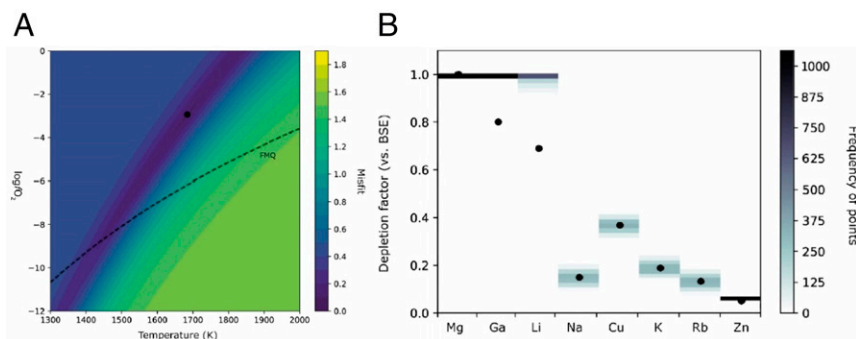


Fig. 3. Calculated physical conditions of MVE depletions in the BLM, and MVE depletion factors *f*. (A) The minimization surface contoured by the misfit to the objective function for elemental depletion factors *f* calculated by the model and those observed in the Earth and Moon. Lower values (blues) represent better fits to the observed depletion factors, with a minimum occurring at the black point at $T = 1,670$ K and $f_{\text{O}_2} = \text{FMQ} + 2.3$. The dashed line shows the position of the FMQ buffer. (B) Monte Carlo simulations with variable T and f_{O_2} plotted as frequency distributions of depletion factors *f* for 1,000 simulations calculated according to Eq. 1 (Table 1). See text for discussion.

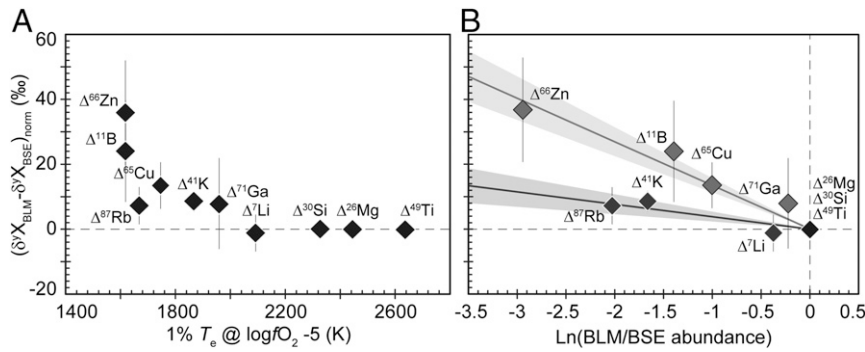


Fig. 4. The difference of stable isotope composition between the BLM and the BSE versus 1% evaporation temperature at $fO_2 \sim FMQ$ at 1,600 to 1,800 K (A) and the BLM/BSE element abundance ratios (B). The stable isotope composition differences are normalized to the mass difference between the two stable isotopes used. For example, $\Delta^{11}B = \text{abs}\{(\delta^{11}B_{BLM} - \delta^{11}B_{BSE}) / [(11 - 10)/10]\}$. The BLM and BSE stable isotope compositions, 1% evaporation temperatures, and BLM/BSE abundance ratios used are given in *SI Appendix, Table S2*.

leave a BLM enriched in lighter K and Rb isotopes compared to the BSE, which is the opposite of what is observed (13, 15, 17, 63).

When plotted against the BLM/BSE element abundance ratios, the isotope enrichment factors between the BLM and the BSE display two distinct trends defined by 1) the alkali metals Li, K, and Rb, and 2) Ga, Cu, B, and Zn, respectively, both passing through the composition of the main component and refractory elements Si, Mg, and Ti (Fig. 4B). This key difference between alkalis and other elements could be related to their different speciation, as alkali metals are always monovalent (1^+), whereas Zn is 2^+ while Ga and B are both present in trivalent form in silicate melts (e.g., ref. 64). Copper could be present as either 1^+ or 2^+ , with the lower valence state predominating for geological conditions (65). Another possibility is that degassing alkali metals formed Cl-bearing gas species (e.g., KCl and RbCl), which would have depressed their gas/melt fractionation factors because these are heavier species in which the metal is more strongly bound with respect to the monatomic gas (e.g., K^0 and Rb^0). Though Cu and Zn may also form chloride species, they are unstable above $\sim 1,000$ K in lunar volcanic gases (52). Importantly, both of these characteristics result from the chemical equilibrium behavior of these elements, arguing against mass transport as the predominant mechanism of isotopic fractionation (see also ref. 66).

If the surface of the LMO is in equilibrium with an overlying vapor, as expected according to physical models of evaporation of rocky bodies (67), the isotopic fractionation factor must be equal to that at equilibrium between liquid and gas at the interface. From our simulations, we determine the temperature to reflect evaporation at $\sim 1,700$ K. Combining these thermal constraints with observed elemental depletions in the BLM relative to the BSE allows the equilibrium isotopic fractionation factor to be calculated. From dynamical models of atmospheric escape, a steady state escaping atmosphere is readily achieved within a timescale of days from evaporating Moon-sized bodies (45, 67). Therefore, because the budget of each element is finite, isotopic fractionation adheres to a Rayleigh distillation mechanism (provided the magma ocean mixing time is fast relative to the escape rate), in which the fractionation factor is given by equilibrium between liquid and gas, which is itself proportional to $1/T^2$. The required equilibrium fractionation factor may be calculated according to

$$10^3 \ln^{ij} \beta_{0,vap} - 10^3 \ln^{ij} \beta_{0,liq} = \frac{T^2}{10^3} \ln \left(\frac{\Delta^i E_{BLM-BSE}}{10^3 \ln f_E} + 1 \right), \quad [4]$$

in which we define $\beta_0 = \beta_{10^6}$, thereby allowing temperature to be solved independently from the beta factor. Here, we use values

of f_E and $\Delta^i E_{BLM-BSE}$ given in *SI Appendix, Tables S1 and S2* and set $T = 1700$ K. Since, for a monatomic gas, $10^3 \ln \beta_{0,vap} = 0$ by definition, Eq. 4 simplifies to

$$10^3 \ln^{ij} \beta_{0,liq} = -\frac{T^2}{10^3} \ln \left(\frac{\Delta^i E_{BLM-BSE}}{10^3 \ln f_E} + 1 \right), \quad [5]$$

whose $10^3 \ln^{ij} \beta_{0,liq}$ value can be directly compared to beta factor coefficients calculated ab initio (e.g., the “b” value of Table 2 of ref. 68). This exercise yields values of $10^3 \ln^{ij} \beta_{0,liq}$ of 1.1‰ for $^{66}/^{64}\text{Zn}$, 1.25‰ for $^{65}/^{63}\text{Cu}$, 0.25‰ for $^{87}/^{85}\text{Rb}$, and 0.65‰ for $^{41}/^{39}\text{K}$, which are equivalent to the beta factors determined in experimental or theoretical studies. These values are a factor of ~ 3 larger than for equilibrium isotope fractionation factors calculated between common minerals and monatomic gas for Zn, K, and Rb (68, 69). In each case, this discrepancy may be remedied by decreasing T from 1,700 K to $\sim 1,200$ K. However, LMO melt is no longer present at these lower temperatures. Nevertheless, the fractionation factors determined through ab initio methods are restricted to mineral–gas reactions, rather than the melt–gas system expected to have led to the volatile loss on the Moon. Whether the minerals represent a good analog for the bonding environment of these elements in the melt remains to be verified. Therefore, while it is thus difficult to exactly satisfy temperature constraints imposed by both the MVE elemental abundances and stable isotope composition differences between the Earth and the Moon, the fractionation factors calculated are in much closer agreement with those determined for solid–gas equilibrium through ab initio methods than for a Langmuir- or diffusion-limited vaporization process (66). Moreover, this exercise illustrates the necessity of considering low temperatures in an equilibrium scenario to account for stable isotope fractionation during vaporization.

Finally, linear regression procedures with direct weighting for the isotope fractionation trend displayed in Fig. 4B yield the relationships $(\delta^i X_{BLM} - \delta^i X_{BSE})_{\text{norm}} = -13.4 (\pm 2.2) \times \ln([X_{BLM}]/[X_{BSE}])$ (95% confidence level) for the nonalkali metals and $(\delta^i X_{BLM} - \delta^i X_{BSE})_{\text{norm}} = -3.8 (\pm 1.5) \times \ln([X_{BLM}]/[X_{BSE}])$ (95% confidence level) for the alkalis Li, K, and Rb. These regressions can be used to predict the stable isotope difference between the BLM and the BSE for a given element, X. For instance, the nonalkali metal relationship predicts that compared to the BSE, the BLM should be fractionated by $+0.7 \pm 0.1\%$ for $^{123}\text{Sb}/^{121}\text{Sb}$ (using $f_{\text{Sb}} = 0.0455$), $+2.4 \pm 0.4\%$ for $^{114}\text{Cd}/^{110}\text{Cd}$ (using $f_{\text{Cd}} = 0.0075$), $+0.6 \pm 0.2\%$ for $^{115}\text{In}/^{113}\text{In}$ (using $f_{\text{In}} = 0.0909$), and $+0.8 \pm 0.3\%$ for $^{82}\text{Se}/^{78}\text{Se}$ (using $f_{\text{Se}} = 0.32$). The latter is consistent with new Se isotope data that indicate that high-Ti mare basalts have $\delta^{82/78}\text{Se} \sim 0.5$ to 0.8%

higher than terrestrial basalts (70). Using the relationship defined by the alkalis for Ag (as Ag is 1+ and typically forms chloride species) predicts $+0.2 \pm 0.1\%$ for $^{109}\text{Ag}/^{107}\text{Ag}$ (using $f_{\text{Ag}} = 0.0375$) in the BLM (using Se lunar mantle abundance from ref. 4 and those from ref. 71 for Sb, Cd, In, and Ag).

Loss of MVEs during a Giant Impact on the Moon Nearside?

Depletions in Na, K, Cr, Cu, Rb, and Zn for sample-derived BLM estimates compared to abundances of these elements in the BSE are consistent with evaporative loss during a large-scale event that took place at $\sim 1,670 \pm 129$ K and an f_{O_2} of FMQ $+2.3 \pm 2.1$. This set of conditions does not uniquely constrain whether MVE depletion and associated isotope fractionation occurred during the protolunar disk cooling stage, during cooling of the LMO before the formation of an insulating lid, or after the formation of a primary crust in response to crust-breaching large-scale event(s). Importantly, samples collected during the Apollo missions are all located within the anomalous PKT region that occupies much of the lunar nearside (72). This whole area could have formed in response to a giant impact event toward the end of the LMO crystallization that led to the formation of the putative Procellarum basin (e.g., ref. 73). Interestingly, results of a recent modeling study suggest that temperatures at the impact site during formation of the Procellarum basin could have been around 2,000 K (74). Moreover, the dynamical lock-up point at which the magma–crystal system transitions from a suspension to a crystal mush (at a porosity of 0.4) is modeled to occur at $\sim 1,700$ K in magma oceans (75, 76). At this point, mass transport within the body is far more sluggish, limiting chemical and thermal transport to the surface. Because the planet continues to cool at a rate proportional to T^4 (a black or gray body), cooling predominates thereafter, effectively arresting vaporization. These temperatures are similar to that at which we estimate MVE to have been partially lost from lunar samples. The MVE depletion in the BLM, and the associated isotope fractionation of MVEs compared to their composition in the BSE, could thus be a direct consequence of the formation of the Procellarum basin early in the Moon's history. In this scenario, the Procellarum-forming giant impact event would have exposed nearside LMO melts at the surface, allowing equilibration with any primitive atmosphere and MVE loss and isotopic fractionation, as proposed by Barnes et al. (26) to explain elevated Cl isotope ratios in KREEP-rich samples. We note that this scenario does not preclude that some volatile element depletions were inherited from the Moon-forming giant impact and protolunar disk cooling but simply demonstrates that such a localized basin-forming event is also permissible unless the whole Moon can be shown to have suffered consistent volatile loss and associated isotope fractionation.

Analyzing samples from outside the Procellarum area on the lunar nearside should allow testing of the scenario proposed here to explain the MVE depletion and associated isotopic fractionation observed in Apollo sample-derived estimates for the BLM composition. BLM estimates derived from non-Procellarum basaltic samples should indeed yield MVE abundances and isotope

compositions consistent with those of the BSE. Unbrecciated basaltic lunar meteorites likely provide us with a random proxy sampling of the Moon's interior. Unfortunately, there are only a dozen or so unbrecciated basaltic meteorite samples, considering pairings (meteorites.wustl.edu/lunar/moon_meteorites_list_alumina.htm), and MVE stable isotope data for only a handful of these. Additionally, precisely pinpointing the location from where lunar meteorites were ejected from the Moon is not straightforward, especially for unbrecciated basalts, since they may have originated from greater depths than those probed by remote sensing instruments (77). Day et al. (47) recently analyzed the Zn abundance and isotope composition of four basaltic meteorites (LaPaz Icefield [LAP] 02205 and Northwest Africa [NWA] 479, NWA 4734, and NWA 8632) and obtained Zn isotope compositions consistent with Apollo mare basalt data. However, these basaltic meteorites contain ~ 1.3 to $2 \mu\text{g} \cdot \text{g}^{-1}$ Th and likely originated from the PKT area (77). LAP 02224 and Miller Range (MIL) 05035 have K isotope compositions consistent with those of Apollo mare basalts (63). If LAP 02224 likely originated from within the PKT area (77), the YAMM meteorite group (which includes Yamato-793169, Asuka-881757, Meteorite Hills 01210, and MIL 05035) may have been launched from Mare Crisium, Mare Fecunditatis, or Mare Humorum, all on the limb of the PKT area (77, 78). Interestingly, their mantle source region might be characterized by much higher Pb/U ratios compared to Apollo mare basalts, comparable to the BSE Pb/U ratio (79, 80). Apatite in MIL 05035 also records lower Cl isotope ratios than apatite in the majority of Apollo mare basalts (25, 81), with $\delta^{37}\text{Cl}$ values between $\sim -4 \pm 2$ and $+7.5 \pm 1.4\%$ and overlapping $\delta^{37}\text{Cl}$ values typical of terrestrial basalts (82). Some of the characteristics of the YAMM meteorites, such as Pb/U or Cl isotope ratios, thus appear more consistent with terrestrial characteristics, while others, such as the K isotope composition of MIL 05035, are akin to the K isotope composition of Apollo mare basalts. The sparse existing MVE dataset on unbrecciated basaltic meteorites, together with the difficulty in pinpointing where on the Moon these samples came from, prevent further evaluation of our proposed hypothesis at present. To do so, MVE abundance and isotope analyses are needed from basaltic samples from well outside the PKT area on the lunar nearside. In this respect, targeting basaltic lava flows in areas of the Moon away from the Procellarum basin should be a high priority for future lunar sample return missions.

Data Availability. All study data are included in the article and/or *SI Appendix*.

ACKNOWLEDGMENTS. We thank Dr. Katherine Joy for her insightful suggestions on an earlier version of this manuscript and two anonymous reviewers for their comments and suggestions that helped us improve this manuscript. R.T. acknowledges the UK Science and Technology Facilities Council for financial support (Grant #ST/P005225/1). P.A.S. acknowledges support from Swiss National Science Foundation Ambizione Fellowship grant #180025. F.M. acknowledges funding from the European Research Council (ERC) under the H2020 framework program/ERC Grant Agreement No. 637503 (Pristine) and financial support of the UnivEarthS Labex program at Sorbonne Paris Cité (ANR-10-LABX-0023 and ANR-11-IDEX-0005-02).

1. A. E. Ringwood, S. E. Kesson, Basaltic magmatism and the bulk composition of the Moon. *Earth Moon Planets* **16**, 425–464 (1977).
2. R. Wolf, E. Anders, Moon and Earth: Compositional differences inferred from siderophiles, volatiles, and alkalis in basalts. *Geochim. Cosmochim. Acta* **44**, 2111–2124 (1980).
3. A. E. Saal et al., Volatile content of lunar volcanic glasses and the presence of water in the Moon's interior. *Nature* **454**, 192–195 (2008).
4. E. H. Hauri, A. E. Saal, M. J. Rutherford, J. A. Van Orman, Water in the Moon's interior: Truth and consequences. *Earth Planet. Sci. Lett.* **409**, 252–264 (2015).
5. F. M. McCubbin et al., Magmatic volatiles (H, C, N, F, S, Cl) in the lunar mantle, crust, and regolith: Abundances, distributions, processes, and reservoirs. *Am. Mineral.* **100**, 1668–1707 (2015).

6. K. Lodders, Solar system Abundances and condensation temperatures of the elements. *Astrophys. J.* **591**, 1220–1247 (2003).
7. F. Moynier, F. Albarède, G. F. Herzog, Isotopic composition of zinc and copper in lunar samples. *Geochim. Cosmochim. Acta* **70**, 6103–6117 (2006).
8. G. F. Herzog, F. Moynier, F. Albarède, A. A. Berezhnoy, Isotopic and elemental abundances of copper and zinc in lunar samples, Zagami, Pele's hairs, and a terrestrial basalt. *Geochim. Cosmochim. Acta* **73**, 5884–5904 (2009).
9. R. C. Paniello, J. M. D. Day, F. Moynier, Zinc isotopic evidence for the origin of the Moon. *Nature* **490**, 376–379 (2012).
10. E. Füri, P. H. Barry, L. A. Taylor, B. Marty, Indigenous nitrogen in the Moon: Constraints from coupled nitrogen–noble gas analyses of mare basalts. *Earth Planet. Sci. Lett.* **431**, 195–205 (2015).

11. C. Kato, F. Moynier, M. C. Valdes, J. K. Dhaliwal, J. M. D. Day, Extensive volatile loss during formation and differentiation of the Moon. *Nat. Commun.* **6**, 7617 (2015).
12. J. Mortimer, A. B. Verchovsky, M. Anand, I. Gilmour, C. T. Pillinger, Simultaneous analysis of abundance and isotopic composition of nitrogen, carbon, and noble gases in lunar basalts: Insights into interior and surface processes on the Moon. *Icarus* **255**, 3–17 (2015).
13. K. Wang, S. B. Jacobsen, Potassium isotopic evidence for a high-energy giant impact origin of the Moon. *Nature* **538**, 487–490 (2016).
14. C. Kato, F. Moynier, Gallium isotopic evidence for extensive volatile loss from the Moon during its formation. *Sci. Adv.* **3**, e1700571 (2017).
15. E. Pringle, F. Moynier, Rubidium isotopic composition of the Earth, meteorites, and the Moon: Evidence for the origin of volatile loss during planetary accretion. *Earth Planet. Sci. Lett.* **473**, 62–70 (2017).
16. P. A. Sossi, F. Moynier, K. van Zuilen, Volatile loss following cooling and accretion of the Moon revealed by chromium isotopes. *Proc. Natl. Acad. Sci. U.S.A.* **115**, 10920–10925 (2018).
17. N. X. Nie, N. Dauphas, Vapor drainage in the protolunar disk as the cause for the depletion in volatile elements of the moon. *Astrophys. J.* **884**, L48 (2019).
18. X. Wang, C. Fitoussi, B. Bourdon, B. Fegley, Jr, S. Charnoz, Tin isotopes indicative of liquid–vapour equilibration and separation in the Moon-forming disk. *Nat. Geosci.* **12**, 707–711 (2019).
19. J. W. Boyce et al., Lunar apatite with terrestrial volatile abundances. *Nature* **466**, 466–469 (2010).
20. F. M. McCubbin et al., Nominally hydrous magmatism on the Moon. *Proc. Natl. Acad. Sci. U.S.A.* **107**, 11223–11228 (2010).
21. J. P. Greenwood et al., Hydrogen isotope ratios in lunar rocks indicate delivery of cometary water to the Moon. *Nat. Geosci.* **4**, 79–82 (2011).
22. R. Tartèse et al., The abundance, distribution, and isotopic composition of hydrogen in the moon as revealed by basaltic lunar samples: Implications for the volatile inventory of the moon. *Geochim. Cosmochim. Acta* **122**, 58–74 (2013).
23. A. E. Saal, E. H. Hauri, J. A. Van Orman, M. J. Rutherford, Hydrogen isotopes in lunar volcanic glasses and melt inclusions reveal a carbonaceous chondrite heritage. *Science* **340**, 1317–1320 (2013).
24. D. T. Wetzel, E. H. Hauri, A. E. Saal, M. J. Rutherford, Carbon content and degassing history of the lunar volcanic glasses. *Nat. Geosci.* **8**, 755–758 (2015).
25. J. W. Boyce et al., The chlorine isotope fingerprint of the lunar magma ocean. *Sci. Adv.* **1**, e1500380 (2015).
26. J. J. Barnes et al., Early degassing of lunar urKREEP by crust-breaching impact(s). *Earth Planet. Sci. Lett.* **447**, 84–94 (2016).
27. P. Ni, Y. Zhang, S. Chen, J. Gagnon, A melt inclusion study on volatile abundances in the lunar mantle. *Geochim. Cosmochim. Acta* **249**, 17–41 (2019).
28. A. Stephant et al., The hydrogen isotopic composition of lunar melt inclusions: An interplay of complex magmatic and secondary processes. *Geochim. Cosmochim. Acta* **284**, 196–221 (2020).
29. R. M. Canup, C. Visscher, J. Salmon, B. Fegley Jr, Depletion of volatile elements in the Moon due to incomplete accretion within an impact-generated disk. *Nat. Geosci.* **8**, 918–921 (2015).
30. S. J. Lock et al., The origin of the moon within a terrestrial synestia. *J. Geophys. Res. Planets* **123**, 910–951 (2018).
31. J. M. D. Day, F. Moynier, Evaporative fractionation of volatile stable isotopes and their bearing on the origin of the Moon. *Philos. Trans. Roy. Soc. Math. Phys. Eng. Sci.* **372**, 20130259 (2014).
32. R. Tartèse et al., Constraining the evolutionary history of the moon and the inner solar system: A case for new returned lunar samples. *Space Sci. Rev.* **215**, 54 (2019).
33. H. C. Urey, Chemical fractionation in the meteorites and the abundance of the element. *Geochim. Cosmochim. Acta* **2**, 269–282 (1952).
34. L. Grossman, J. W. Larimer, Early chemical history of the solar system. *Rev. Geophys. Space Phys.* **12**, 71–101 (1974).
35. P. A. Sossi, S. Klemme, H. O'Neill, J. Berndt, F. Moynier, Evaporation of moderately volatile elements from silicate melts: Experiments and theory. *Geochim. Cosmochim. Acta* **260**, 204–231 (2019).
36. H. S. C. O'Neill, H. Palme, Collisional erosion and the non-chondritic composition of the terrestrial planets. *Philos. Trans. Roy. Soc. Math. Phys. Eng. Sci.* **366**, 4205–4238 (2008).
37. C. A. Norris, B. J. Wood, Earth's volatile contents established by melting and vaporization. *Nature* **549**, 507–510 (2017).
38. P. L. Clay et al., Halogens in chondritic meteorites and terrestrial accretion. *Nature* **551**, 614–618 (2017).
39. B. J. Wood, D. J. Smythe, T. Harrison, The condensation temperatures of the elements: A reappraisal. *Am. Mineral.* **104**, 844–856 (2019).
40. M. J. O'Hara, G. M. Biggar, S. W. Richardson, C. E. Ford, B. G. Jamieson, "The nature of seas, mascons and the lunar interior in the light of experimental studies" in *Proc. Apollo 11 Lunar Sci. Conf. 1* (Pergamon Press, New York, 1970), pp. 695–710.
41. J. T. Wasson, W. V. Boynton, G. W. Kallemeyn, L. L. Sundberg, C. M. Wai, "Volatile compounds released during lunar lava fountaining" in *Proc. Seventh Lunar Sci. Conf.* (Pergamon Press, New York, 1976), pp. 1583–1595.
42. F. Albarède, E. Albalat, C. A. Lee, An intrinsic volatility scale relevant to the Earth and Moon and the status of water in the Moon. *Meteorit. Planet. Sci.* **50**, 568–577 (2015).
43. M. M. Hirschmann, Constraints on the early delivery and fractionation of Earth's major volatiles from C/H, C/N and C/S ratios. *Am. Mineral.* **101**, 540–553 (2016).
44. H. E. Schlichting, S. Mukhopadhyay, Atmosphere impact losses. *Space Sci. Rev.* **214**, 34 (2018).
45. S. Charnoz et al., "Efficient early Moon devolatilisation just after its formation, through tidally-assisted hydrodynamic escape" in 50th Lunar Planet. Sci. Conf., abstr. #2395 (2019). <https://www.hou.usra.edu/meetings/lpsc2019/pdf/2395.pdf>. Accessed 25 February 2021.
46. E. D. Young et al., Near-equilibrium isotope fractionation during planetesimal evaporation. *Icarus* **323**, 1–15 (2019).
47. J. M. D. Day, E. M. M. E. van Kooten, N. A. Hofmann, F. Moynier, Mare basalt meteorites, magnesian-suite rocks and KREEP reveal loss of zinc during and after lunar formation. *Earth Planet. Sci. Lett.* **531**, 115998 (2020).
48. U. Mann, D. J. Frost, D. C. Rubie, Evidence for high-pressure core-mantle differentiation from the metal-silicate partitioning of lithophile and weakly-siderophile elements. *Geochim. Cosmochim. Acta* **73**, 7360–7386 (2009).
49. B. Mahan et al., Constraining compositional proxies for the Earth's accretion and core formation through high pressure and high temperature Zn and S metal silicate partitioning. *Geochim. Cosmochim. Acta* **235**, 21–40 (2018).
50. Y. Xia, E. S. Kiseeva, J. Wade, F. Huang, The effect of core segregation on the Cu and Zn isotope composition of the silicate Moon. *Geochem. Perspect. Lett.* **12**, 12–17 (2019).
51. R. H. Lamoreaux, D. L. Hildenbrand, L. Brewer, High-temperature vaporization behavior of oxides II. Oxides of Be, Mg, Ca, Sr, Ba, B, Al, Ga, In, Tl, Si, Ge, Sn, Pb, Zn, Cd, and Hg. *J. Phys. Chem. Ref. Data* **16**, 419–443 (1987).
52. C. J. Renggli, P. L. King, R. W. Henley, M. D. Norman, Volcanic gas composition, metal dispersion and deposition during explosive volcanic eruptions on the Moon. *Geochim. Cosmochim. Acta* **206**, 296–311 (2017).
53. M. Wadhwa, Redox conditions on small bodies, the moon and Mars. *Rev. Mineral. Geochem.* **68**, 493–510 (2008).
54. J. F. Rapp, D. S. Draper, Fractional crystallization of the lunar magma ocean: Updating the dominant paradigm. *Meteorit. Planet. Sci.* **53**, 1432–1455 (2018).
55. T. Mikouchi, N. Yokoi, A. Takenouchi, T. Arai, "High oxygen fugacity of lunar anorthosites as revealed by iron micro-XANES of plagioclase" in 50th Lunar Planet. Sci. Conf., abstr. #2341 (2019). <https://www.hou.usra.edu/meetings/lpsc2019/pdf/2341.pdf>. Accessed 25 February 2021.
56. G. De Maria, G. Balducci, M. Guido, V. Piacente, "Mass spectrometric investigation of the vaporization process of Apollo 12 lunar samples" in *Proc. Second. Lunar Sci. Conf. 2* (The MIT Press, Cambridge, 1971), pp. 1367–1380.
57. C. Visscher, B. Fegley, Chemistry of impact-generated silicate melt–vapor debris disks. *Astrophys. J.* **767**, L12 (2013).
58. B. J. Wood, E. S. Kiseeva, F. J. Mirolo, Accretion and core formation: The effects of sulfur on metal-silicate partition coefficients. *Geochim. Cosmochim. Acta* **145**, 248–267 (2014).
59. H. St. C. O'Neill, The origin of the moon and the early history of the earth—A chemical model. Part 1: The moon. *Geochim. Cosmochim. Acta* **55**, 1135–1157 (1991).
60. J. M. D. Day et al., Evidence for high-temperature fractionation of lithium isotopes during differentiation of the Moon. *Meteorit. Planet. Sci.* **51**, 1046–1062 (2016).
61. E. S. Steenstra, N. Rai, J. S. Knibbe, Y. H. Lin, W. van Westrenen, New geochemical models of core formation in the Moon from metal-silicate partitioning of 15 siderophile elements. *Earth Planet. Sci. Lett.* **441**, 1–9 (2016).
62. J. K. Dhaliwal, J. M. D. Day, F. Moynier, Volatile element loss during planetary magma ocean phases. *Icarus* **300**, 249–260 (2018).
63. Z. Tian et al., Potassium isotopic composition of the Moon. *Geochim. Cosmochim. Acta* **280**, 263–280 (2020).
64. P. C. Hess, "The role of high field strength cations in silicate melts" in *Physical Chemistry of Magmas. Advances in Physical Geochemistry*, L. L. Perchuk, I. Kushiro, Eds. (Springer, New York, NY, 1991), vol. 9.
65. A. Holzheid, K. Lodders, Solubility of copper in silicate melts as function of oxygen and sulfur fugacities, temperature, and silicate composition. *Geochim. Cosmochim. Acta* **65**, 1933–1951 (2001).
66. P. A. Sossi et al., An experimentally-determined general formalism for evaporation and isotope fractionation of Cu and Zn from silicate melts between 1300 and 1500 °C and 1 bar. *Geochim. Cosmochim. Acta* **288**, 316–340 (2020).
67. H. Tang, E. D. Young, Evaporation from the lunar Magma Ocean was not the mechanism for fractionation of the Moon's moderately volatile elements. *Planet. Sci. J.* **1**, 49 (2020).
68. M. Ducher, M. Blanchard, E. Balan, Equilibrium zinc isotope fractionation in Zn-bearing minerals from first-principles calculations. *Chem. Geol.* **443**, 87–96 (2016).
69. H. Zeng et al., Ab initio calculation of equilibrium isotopic fractionations of potassium and rubidium in minerals and water. *ACS Earth Space Chem.* **3**, 2601–2612 (2019).

70. H. Vollstaedt, K. Mezger, I. Leya, The selenium isotope composition of lunar rocks: Implications for the formation of the Moon and its volatile loss. *Earth Planet. Sci. Lett.* **542**, 116289 (2020).
71. K. Richter, Volatile element depletion of the Moon-The roles of precursors, post-impact disk dynamics, and core formation. *Sci. Adv.* **5**, eaau7658 (2019).
72. B. L. Jolliff *et al.*, Major lunar crustal terranes: Surface expressions and crust-mantle origins. *J. Geophys. Res. Planets* **105**, 4197–4216 (2000).
73. E. A. Whitaker, The lunar Procellarum basin. *Proc. Lunar Planet. Sci.* **12A**, 105–111 (1981).
74. M. H. Zhu, K. Wünnemann, R. W. K. Potter, T. Kleine, A. Morbidelli, Are the Moon's nearside-farside asymmetries the result of a giant impact? *J. Geophys. Res. Planets* **124**, 2117–2140 (2019).
75. D. J. Bower *et al.*, Linking the evolution of terrestrial interiors and an early out-gassed atmosphere to astrophysical observations. *Astron. Astrophys.* **631**, A103 (2019).
76. A. Nikolaou *et al.*, What factors affect the duration and outgassing of the terrestrial magma ocean? *Astrophys. J.* **875**, 11 (2019).
77. A. Calzada-Diaz, K. H. Joy, I. A. Crawford, T. A. Nordheim, Constraining the source regions of lunar meteorites using orbital geochemical data. *Meteorit. Planet. Sci.* **50**, 214–228 (2015).
78. K. H. Joy *et al.*, The petrology and geochemistry of Miller range 05035: A new lunar gabbroic meteorite. *Geochim. Cosmochim. Acta* **72**, 3822–3844 (2008).
79. K. Misawa, M. Tatsumoto, G. B. Dalrymple, K. Yanai, An extremely low U/Pb source in the moon: U-Th-Pb, Sm-Nd, Rb-Sr, and $^{40}\text{Ar}/^{39}\text{Ar}$ isotopic systematics and age of lunar meteorite Asuka 881757. *Geochim. Cosmochim. Acta* **57**, 4687–4702 (1993).
80. K. Terada, Y. Sasaki, M. Anand, K. H. Joy, Y. Sano, Uranium-lead systematics of phosphates in lunar basaltic regolith breccia, Meteorite Hills 01210. *Earth Planet. Sci. Lett.* **259**, 77–84 (2007).
81. J. J. Barnes, I. A. Franchi, F. M. McCubbin, M. Anand, Multiple reservoirs of volatiles in the Moon revealed by the isotopic composition of chlorine in lunar basalts. *Geochim. Cosmochim. Acta* **266**, 144–162 (2019).
82. Z. D. Sharp *et al.*, The chlorine isotope composition of chondrites and Earth. *Geochim. Cosmochim. Acta* **107**, 189–204 (2013).